

Featured Article

Invited Review

The potential of organoids in toxicologic pathology: Histopathological and immunohistochemical evaluation of a mouse normal tissue-derived organoid-based carcinogenesis model

Rikako Ishigamori¹, Mie Naruse¹, Akihiro Hirata³, Yoshiaki Maru⁴, Yoshitaka Hippo⁴, and Toshio Imai^{1,2*}

¹ Central Animal Division, National Cancer Center Research Institute, 5-1-1 Tsukiji, Chuo-ku, Tokyo 104-0045 Japan

² Department of Cancer Model Development, National Cancer Center Research Institute, 5-1-1 Tsukiji, Chuo-ku, Tokyo 104-0045 Japan

³ Laboratory of Veterinary Pathology, Joint Department of Veterinary Medicine, Faculty of Applied Biological Sciences, Gifu University, 1-1 Yanagido, Gifu 501-1193, Japan

⁴ Department of Molecular Carcinogenesis, Chiba Cancer Center Research Institute, 666-2 Nitonacho, Chuo-ku, Chiba 260-8717, Japan

Abstract: Recently, we introduced an organoid-based chemical carcinogenesis model using mouse normal tissue-derived organoids. In the present review article, the histopathological and immunohistochemical characteristics of mouse normal tissue-derived organoids and tumors derived from these organoids after their *in vitro* treatment with genotoxic carcinogens and injection into nude mouse are reviewed. In organoids treated *in vitro* with genotoxic carcinogens, we confirmed macroscopic tumorigenicity and histopathological findings, including neoplastic characteristics, such as multilayered epithelia and/or invasion of epithelia into the surrounding interstitium. In contrast glandular/cystic structures with monolayered epithelia were clearly demarcated from the surrounding Matrigel/interstitium in the untreated control groups. In addition to macroscopic tumorigenicity, these microscopic epithelial changes, which are characteristic of the early stages of carcinogenesis, are included in the requirements for carcinogenicity-positive judgement of the organoid-based carcinogenesis model. Immunohistochemistry of cytokeratins (CKs), used to determine the origin of epithelia and distribution of extraductal invasive lesions, or oncogenic kinases, which reflect molecular activation in epithelia following chemical treatment, is helpful for accurate diagnosis and molecular evaluation in the early stages of carcinogenesis. This information improves our biological understanding of organoid-based chemical carcinogenesis models. (DOI: 10.1293/tox.2022-0021; J Toxicol Pathol 2022; 35: 211–223)

Key words: organoids, mouse, carcinogenesis, carcinogen, cytokeratins, kinases

Introduction

The carcinogenic potential of chemicals was first acknowledged by the US National Cancer Institute in the late 1960s. In 1978, the National Toxicology Program was established, which examines chemical-induced carcinogenesis mostly in groups of male and female rats and mice exposed to a chemical for two years¹. Since the 2000s, in addition to long-term studies focusing on continuous administration of test chemicals, several alternative medium-term models

for examining carcinogenicity of chemicals established using genetically engineered mice (GEM), for example, *rash2* mice, have been introduced^{2–5}. In addition, established animal carcinogenesis models treated with certain classes of chemical carcinogens have been frequently used not only for hazard assessment of chemicals, but also for preclinical evaluation of potential chemopreventive agents^{6,7}. These test systems using rats and mice remain the cornerstone for the identification of chemical carcinogens and chemopreventive agents. However, these approaches, particularly long-term studies, are time-consuming, use a large number of animals, and include the continuous administration of test chemicals at maximal tolerated doses *in vivo*^{8,9}. Therefore, the development of alternative models in which chemicals are treated *in vitro*, the duration and number of animals can be reduced, and histopathology as an end-point of evaluation has been awaited.

A three-dimensional (3D) cell culture system has enabled the maintenance of normal tissue-derived cells for at least 10–20 weeks *in vitro*. The organoid culture system was

Received: 16 February 2022, Accepted: 28 March 2022

Published online in J-STAGE: 22 April 2022

*Corresponding author: T Imai

(e-mail: toimai@ncc.go.jp)

©2022 The Japanese Society of Toxicologic Pathology

This is an open-access article distributed under the terms of the Creative Commons Attribution Non-Commercial No Derivatives

(by-nc-nd) License. (CC-BY-NC-ND 4.0: <https://creativecommons.org/licenses/by-nc-nd/4.0/>).



first reported by Sato *et al.* using normal intestinal epithelia in 2009¹⁰, and organoids from different human/mouse organs and tissues, including the lung¹¹, liver¹², and kidney¹³, have been introduced to date. Normal organ/tissue-derived organoids consist of differentiated cells such as enterocytes, goblet cells, Paneth cells, and enteroendocrine cells of the intestine¹⁰, and ciliated cells, goblet cells, and club cells of the lungs¹¹. Human organoids are expected to mimic many *in vivo* physiological functions of relevant tissues, thus filling the translational gap between animals and humans. However, the number of toxicity studies using human organoids remains limited¹⁴. As an application of normal murine organ/tissue-derived organoids, we reported sequential cancer-related gene alterations in intestinal organoids, transduced with lentivirus-based RNAi that mediated knockdown of tumor suppressor genes or activation of Kras, which evolved in adenocarcinomas after their injection into nude mouse subcutis¹⁵. The genetic reconstitution model recapitulated the stepwise carcinogenesis process through the accumulation of multiple genetic alterations in the primary murine intestinal cells. Similar phenomena have been induced in human intestinal cells using CRISPR/Cas9-mediated gene editing^{16, 17} and other organ/tissue-derived organoids^{18–20}.

We recently reported an organoid-based chemical carcinogenesis model established using mouse normal tissue-derived organoids²¹. In this report, four genotoxic chemicals (acrylamide [AA], diethylnitrosamine [DEN], ethyl methanesulfonate [EMS], and 7,12-dimethylbenz[*a*]anthracene [DMBA]) were used to treat normal lung, liver (biliary tract), and/or mammary tissue-derived organoids with a heterozygous *Trp53* knockout background *in vitro* to examine their tumorigenicity after injection into nude mice. The four chemicals induced tumorigenicity or carcinogenic histopathological characteristics with the activation of oncogenic kinases, consistent with previous reports in corresponding animal studies. More recently, DMBA-treated mammary organoids developed into tumors after their injection into nude mouse subcutis were genetically analyzed, and unique changes from a corresponding *in vivo* carcinogenesis model were found. This suggests that organoid-based carcinogenesis models treated with chemicals *in vitro* can be applied to detect early genetic events and/or clarify novel modes of action of chemical carcinogenesis²². Although further validation studies are needed to clarify whether the organoid-based chemical carcinogenesis model is suitable for screening the carcinogenic potential of genotoxic chemicals, this system is a potential candidate method for the evaluation of chemicals as it is short-term, requires a small number of animals, and has a histopathologically-based endpoint of evaluation.

In the present review article, histopathological and immunohistochemical characteristics of mouse normal tissue-derived organoids and tumors developed from chemically treated organoids after their injection into nude mouse subcutis are presented, focusing on the expression of cytokeratins (CKs), which reflect the origin of epithelia and distribution of extraductal invasive lesions, in relation to

the histopathological features. In addition, the expression of oncogenic kinases, which are immunohistochemical markers of the early stages of carcinogenesis that indicate molecular activation in the epithelia after chemical treatment, was analyzed. This information will improve our biological understanding of organoid-based chemical carcinogenesis models.

Methods for Organoid Culturing and Exposure of Chemicals

Organoids are generally produced by culturing epithelial cells/crypts dissociated enzymatically or in the presence of calcium chelators, followed by seeding of the cells/crypts in laminin-rich Matrigel or other basement membrane extracts to support their growth¹⁰. Intestinal organoids grow in culture media containing epidermal growth factor (EGF) for epithelial proliferation, WNT agonists for crypt growth, and Noggin for crypt number expansion¹⁰. Fibroblast growth factors (FGFs) are required to promote formation of lung organoids²³. Organoids from other organs and tissues may have different culture requirements. Dissociated epithelial cells or organoids suspended in Matrigel have been reported to be resistant to lentiviral infection¹⁵ and are considered to be partly resistant to exposed chemicals. Thus, we established a Matrigel bilayer organoid culture method (MBOC) to generate appropriate conditions for the exposure of dissociated epithelial cells to lentivirus and test chemicals²⁴. In MBOC, dissociated epithelial cells are first disseminated on a preformed Matrigel layer in multi-well plates. They are co-cultured overnight with viral particles or test chemicals in culture media. Chemical treatment is performed by mixing culture media with S9 mix for metabolic activation when necessary²¹. The next day, culture media with virus/chemical and floating dead cells are removed, the attached cells are covered with additional Matrigel, and fresh culture media is added for growth. This results in the growth of organoids with cystic/balloon structures in many cases (Fig. 1). Although almost all low-molecular-weight compounds are thought to penetrate the Matrigel layer, exposure of dissociated epithelial cells to test chemicals can be surely achieved during the establishment or passaging of organoids using MBOC.

Subcutaneous Injection of Chemically Treated Organoids into Nude Mice

To evaluate the tumorigenic potential of genetically reconstituted intestinal organoids, lentiviral-transduced organoids were injected into nude mouse subcutis, followed by the preparation of formalin-fixed, paraffin-embedded (FFPE) tissue sections and histopathological evaluation using light microscopy¹⁵. The use of light microscopy for the evaluation of the organoid-derived tissues after injection enabled reliable analysis of the genetic constitutions; in contrast to the use of an inverted microscope which may not be effective to analyze even morphological changes in or-

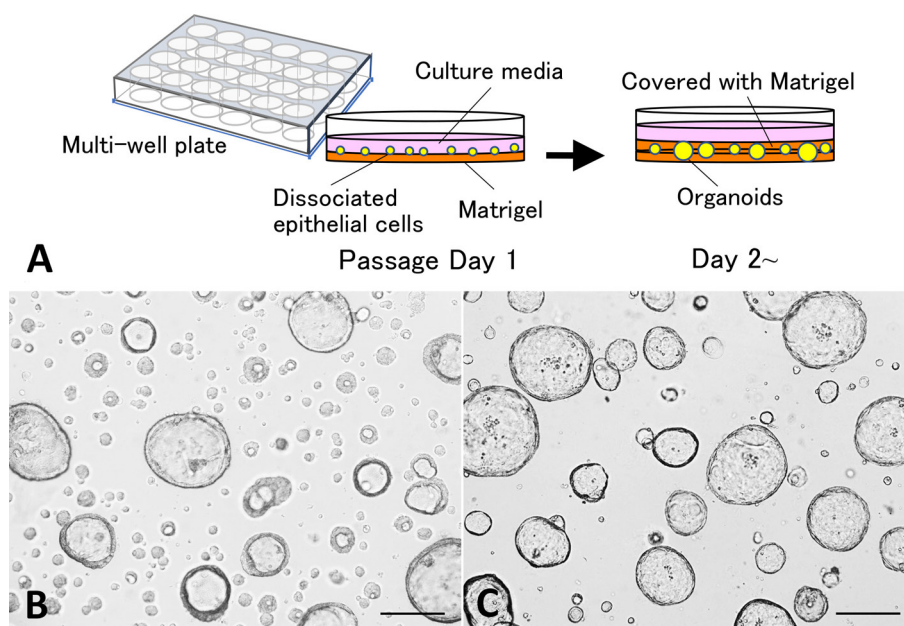


Fig. 1. (A) Illustration of the Matrigel bilayer organoid culture method. (B) Lung organoids derived from a male B6J-wild type mouse in the control group, bar=100 μm . (C) Liver (intrahepatic bile duct) organoids derived from a male B6J-*Trp53* knockout mouse in the control group, bar=100 μm . B6J, C57BL/6J.

ganoids¹⁵. The subcutaneous tissues derived from organoids of not only the intestines, but also the lung²⁵, pancreas¹⁸ and hepatobiliary tract²⁶, with and without genetic reconstitution, were reported to demonstrate focal lesions with different histopathological characteristics, including 1) Matrigel plugs containing microscopic round glandular organoids or no epithelial cells, 2) non-tumorous nodules with a few dysplastic tubular glands lined up with monolayered epithelial cells, 3) solid tumors consisting of tubular glands accompanied by stromal infiltration, and 4) large solid tumors with cysts in which tumor glands were densely packed with malignant characteristics²⁴. The microscopic characteristics of each lesion indicated that normal epithelia almost lost their proliferative potential in interstitial tissue filled with weakly eosinophilic Matrigel (Matrigel plugs), and epithelial cells with preneoplastic and/or neoplastic potentials selectively grew in nude mouse subcutis. Transplantation of organoids into mice enabled us to understand the stepwise changes in carcinogenesis via FFPE tissue section-based histopathology analysis. The genetically altered epithelial cells by lentivirus-based RNAi-mediated knockdown, CRISPR/Cas9-mediated gene editing, or treatment with genotoxic carcinogens exhibited clonal expansion and/or progressed to visible tumors in the mouse subcutis due to accelerated carcinogenesis²².

Macroscopic Appearance of Subcutaneous Tissues in Nude Mice Does Not Necessarily Indicate Tumorigenicity of Chemicals

In our previous report on an organoid-based chemical carcinogenesis model established using normal mouse tis-

sue-derived organoids, tumorigenicity of genotoxic carcinogens was macroscopically confirmed in several cases²¹. For example, BALB/c-heterozygous *Trp53* knockout mouse-derived liver (intrahepatic bile duct) organoids treated *in vitro* with EMS exhibited macroscopically visible yellowish solid changes and/or enlargement after injection into nude mouse subcutis²¹. Histopathologically, they featured neoplastic characteristics, such as multilayered epithelia and invasive growth of epithelia, and one was diagnosed as adenocarcinoma (Fig. 2A). BALB/c-heterozygous *Trp53* knockout mouse-derived mammary organoids treated *in vitro* with DMBA macroscopically exhibited tumorigenicity after injection into nude mouse subcutis²¹, and the formation of adenocarcinomas was histopathologically confirmed (Fig. 2D). However, we previously described that brownish or blackish colored changes, reflecting hemorrhage or cystic changes involving blood serum components, do not necessarily reflect the tumorigenic potential of chemicals because they were also observed in the non-treated control²¹. In this review, several cases are presented for which the carcinogenic characteristics were histopathologically observed but were not macroscopically detected. For example, BALB/c-heterozygous *Trp53* knockout mouse-derived lung organoids treated with EMS showed no notable macroscopic changes (Fig. 3A), but microscopically observed multilayered epithelia and invasive growth of epithelia into the surrounding interstitium suggested carcinogenic characteristics (Fig. 3B). In contrast, simple glandular structures with monolayered epithelia were clearly demarcated from the surrounding Matrigel/interstitium in the untreated control groups (Fig. 4A). C57BL/6J (B6J)-heterozygous *Trp53* knockout mouse-derived liver (intrahepatic bile duct) or-

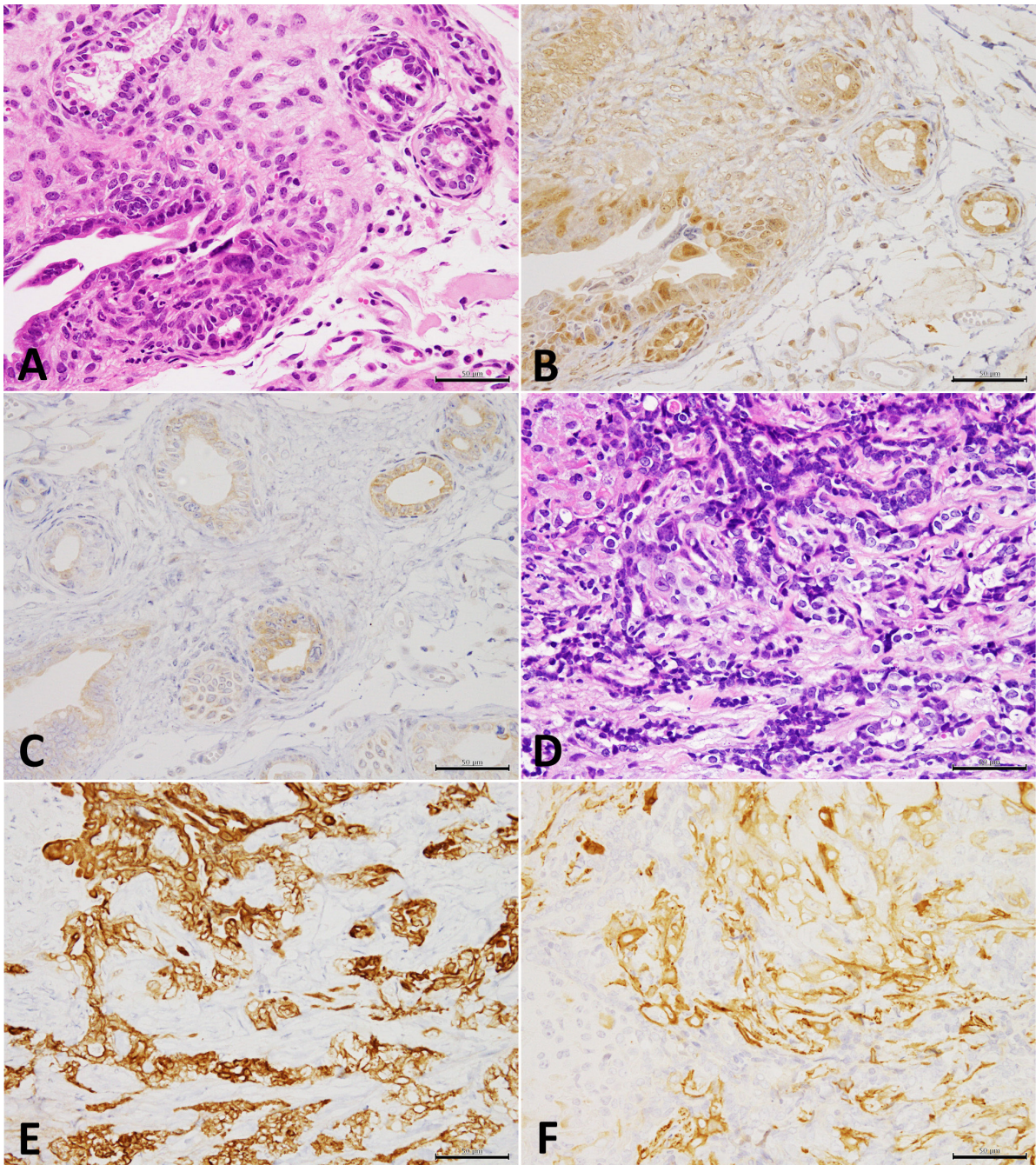


Fig. 2. (A) Adenocarcinoma in the nude mouse subcutis after injection of male BALB/c-heterozygous *Trp53* knockout mouse-derived liver (intrahepatic bile duct) organoids treated with EMS at 0.05 mM. H&E staining, bar=50 μ m. (B) A serial section of (A) immunohistochemically stained for p-ERK1/2. Nuclear positivity was observed in the carcinoma cells. (C) A serial section of (A) immunohistochemically stained for p-Akt. Apical surface/cytoplasmic positivity was observed in the carcinoma cells. (D) Adenocarcinoma in the nude mouse subcutis after injection of female BALB/c-heterozygous *Trp53* knockout mouse-derived mammary organoids treated with DMBA at 0.6 μ M. H&E staining, bar=50 μ m. (E) A serial section of (D) immunohistochemically stained for CK19. Carcinoma cells were positive for CK19. (F) A serial section of (D) immunohistochemically stained for α SMA. α SMA-positive cells surrounding CK19-positive carcinoma cells. DMBA: 7,12-dimethylbenz[a]anthracene; EMS: ethyl methanesulfonate; H&E: hematoxylin and eosin; CK: cytokeratin; α SMA: α smooth muscle actin.

ganoids treated with DEN did not exhibit notable macroscopic changes excluding cystic dilation after injection into the nude mouse subcutis (Fig. 5A); however, histopathological evaluation of the subcutaneous tissues showed irregu-

lar glandular structures with multilayered epithelia in the DEN-treated groups (Fig. 5B). In contrast, simple glandular structures with monolayered epithelia were observed in untreated control groups (Fig. 6A). The EMS- or DEN-treated

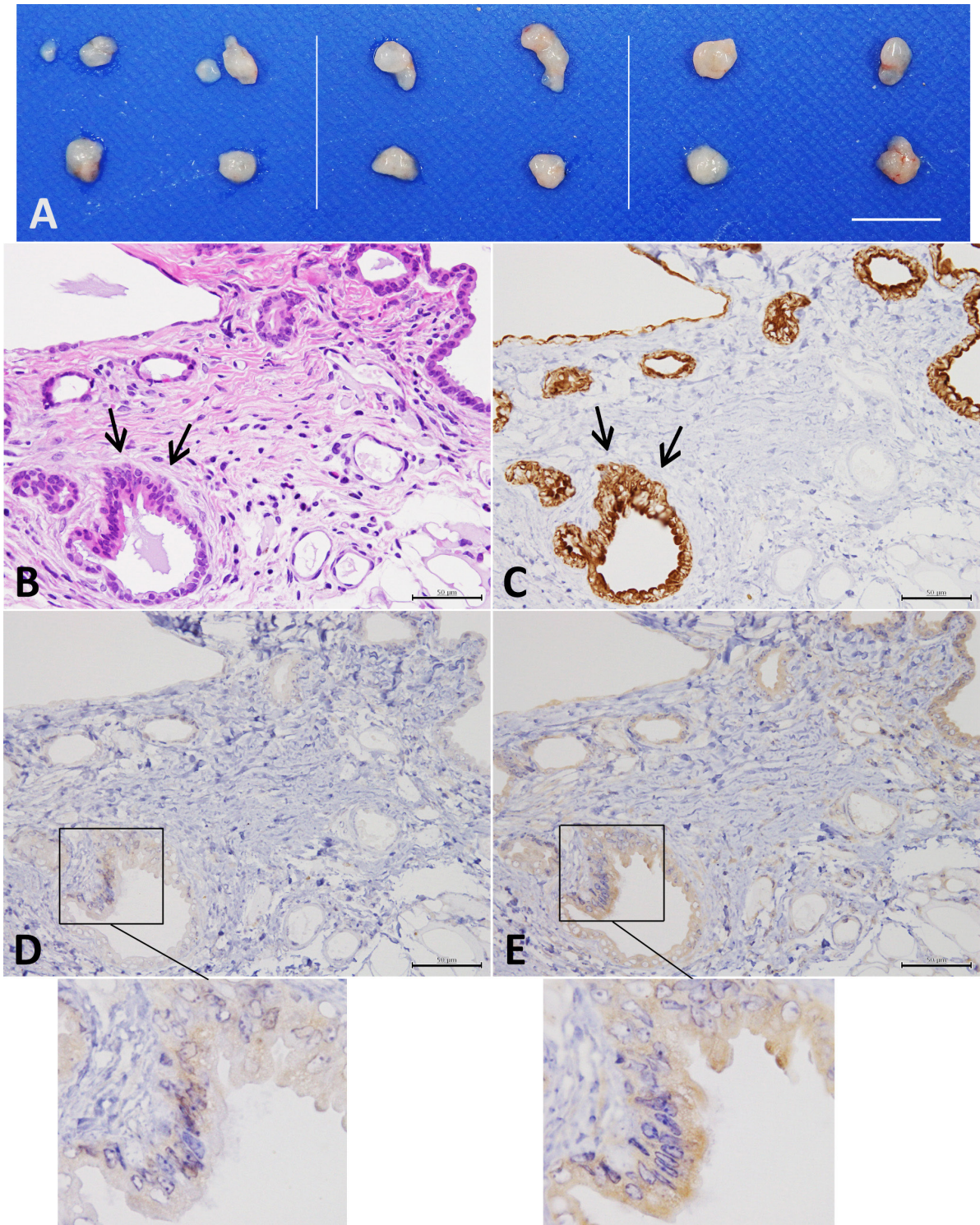


Fig. 3. (A) Macroscopic appearance of Matrigel plugs and non-tumorous nodules in the nude mouse subcutis after injection of male BALB/c-heterozygous *Trp53* knockout mouse-derived lung organoids treated with EMS. Four nodules on the left, EMS 0 mM; four nodules in the middle, EMS 0.05 mM; four nodules on the right, EMS 0.2 mM. No macroscopic changes were observed after EMS treatment. Bar=1 cm. (B) Glandular and cystic structures with partly multilayered epithelia and invasive growth of epithelia into the surrounding interstitium in a nodule of the 0.2 mM EMS-treated group (arrows). H&E staining, bar=50 μ m. (C) A serial section of (B) immunohistochemically stained for CK19. Multilayered epithelia and/or invasion of epithelial cells into the interstitium is shown (arrows). (D) A serial section of (B) immunohistochemically stained for p-ERK1/2. The lower photograph is a higher magnification image of the lower left box. Focal nuclear positivity is observed in the multilayered epithelia. (E) A serial section of (B) immunohistochemically stained for p-Akt. The lower photograph is a higher magnification image of the lower left box. Focal cytoplasmic positivity in the multilayered epithelia is observed. EMS: ethyl methanesulfonate; H&E: hematoxylin and eosin; CK: cytokeratin.

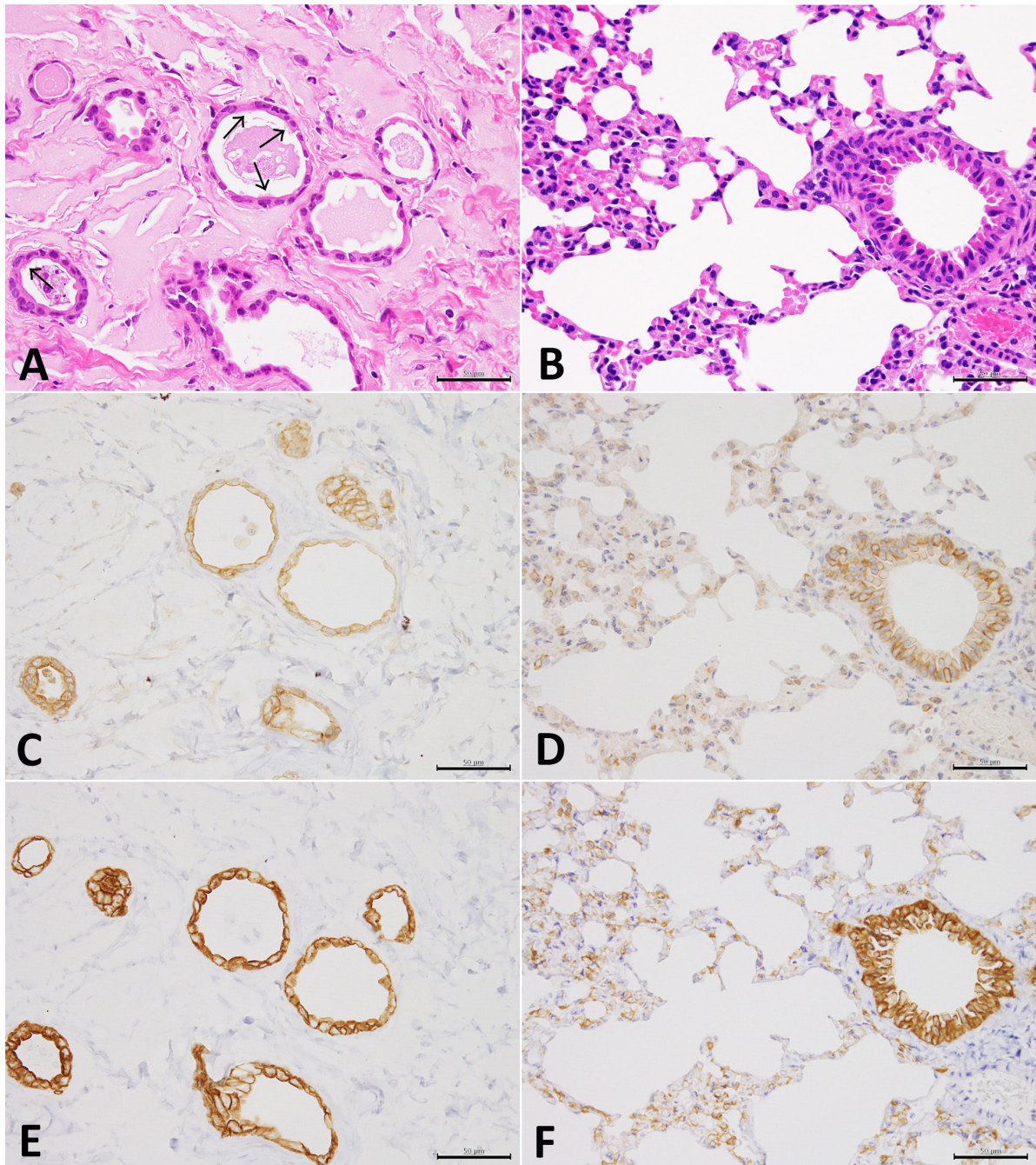


Fig. 4. (A) Microscopic appearance of Matrigel plugs in the nude mouse subcutis after injection of male B6J wild type mouse-derived normal lung organoids. Retained round glandular organoids are found in interstitial tissue filled with retained Matrigel. Arrows; epithelial cells with cilia. H&E staining, bar=50 µm. (B) Lung tissue of normal alveolus and bronchiole of a mouse strain identical to (A). H&E staining, bar=50 µm. (C) A serial section of (A) immunohistochemically stained for CK18. (D) A serial section of (B) immunohistochemically stained for CK18. (E) A serial section of (A) immunohistochemically stained for CK19. Submembranous reactions for CK18/CK19 can be observed in organoid cells. (F) A serial section of (B) immunohistochemically stained for CK19. Submembranous/perinuclear reactions for CK18/CK19 are observed in bronchiolar and alveolar epithelia. B6J: C57BL/6J; H&E: hematoxylin and eosin; CK: cytokeratin.

organoids with multilayered epithelia/invasive growth of epithelia were frequently surrounded by interstitial tissues with fibrous/inflammatory reactions (Figs. 3B and 5B), in contrast to Matrigel plugs, whose interstitium mainly consisted of retained Matrigel in the untreated control groups

(Figs. 4A and 6A). In the evaluation of the mouse normal tissue-derived organoid-based carcinogenesis model, macroscopically observed tumorigenicity and microscopic epithelial changes reflecting the early stages of carcinogenesis are among the requirements for carcinogenicity-positive judge-

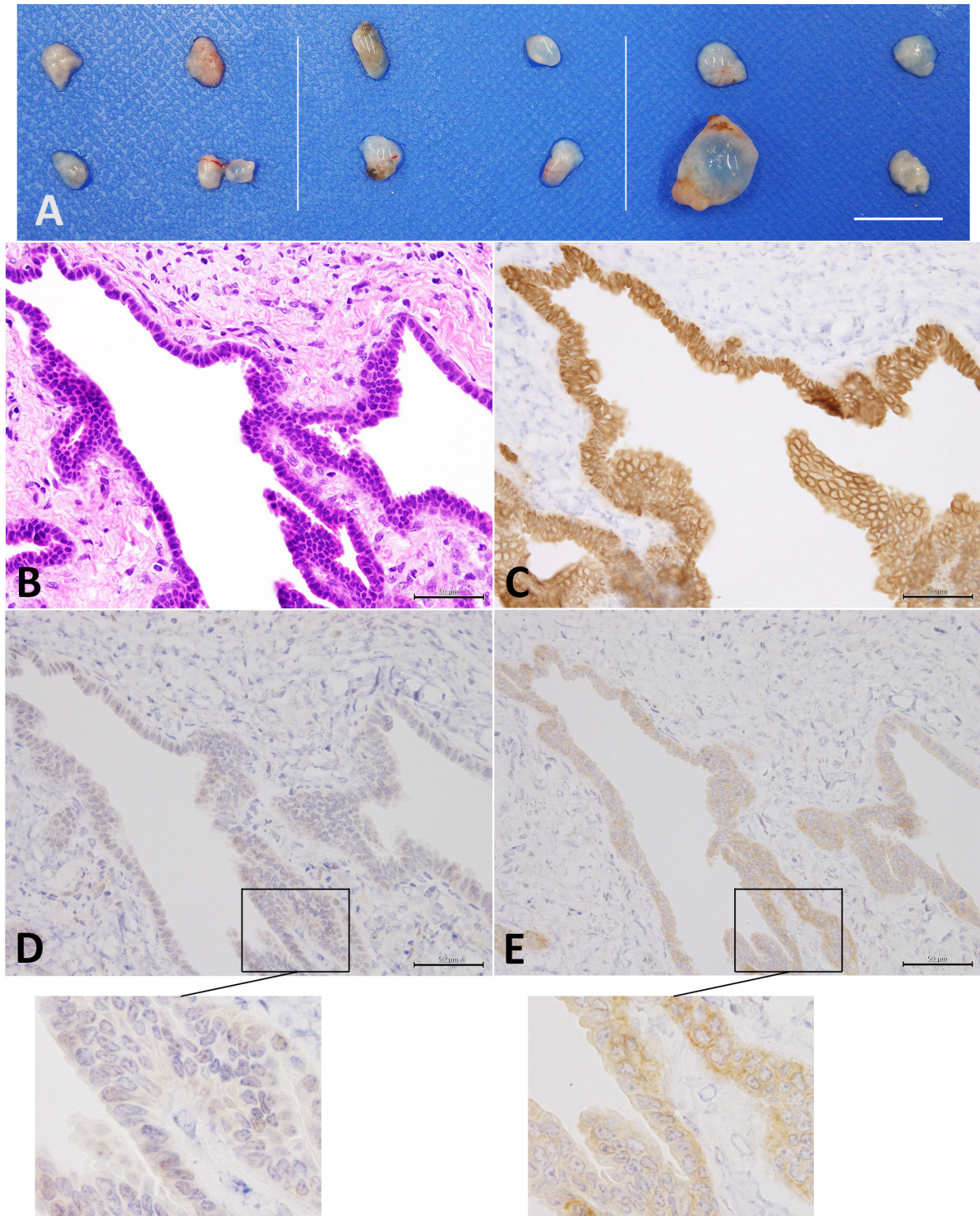


Fig. 5. (A) Macroscopic appearance of Matrigel plugs and non-tumorous nodules in the nude mouse subcutis after injection of male B6J-heterozygous *Trp53* knockout mouse-derived normal liver (intrahepatic bile duct) organoids treated with DEN. Four nodules on the left, DEN 0 mM; four nodules in the middle, DEN 0.2 mM; four nodules on the right, DEN 1.0 mM. No macroscopic changes excluding cystic dilation were observed after DEN treatment. Bar=1 cm. (B) Irregular glandular structures with multilayered epithelia and interstitial fibrous reactions in a nodule in the 0.2 mM DEN-treated group. H&E staining, bar=50 μ m. (C) A serial section of (B) immunohistochemically stained for CK19. Multilayered and/or invasive epithelial cells can be observed. (D) A serial section of (B) immunohistochemically stained for p-ERK1/2. The lower photograph is a higher magnification image of the lower middle box. No reaction was noted. (E) A serial section of (B) immunohistochemically stained for p-Akt. The lower photograph is a higher magnification image of the lower middle box. Cytoplasmic positivity in the multilayered epithelia can be observed. B6J: C57BL/6J; DEN: diethylnitrosamine; H&E: hematoxylin and eosin; CK: cytokeratin.

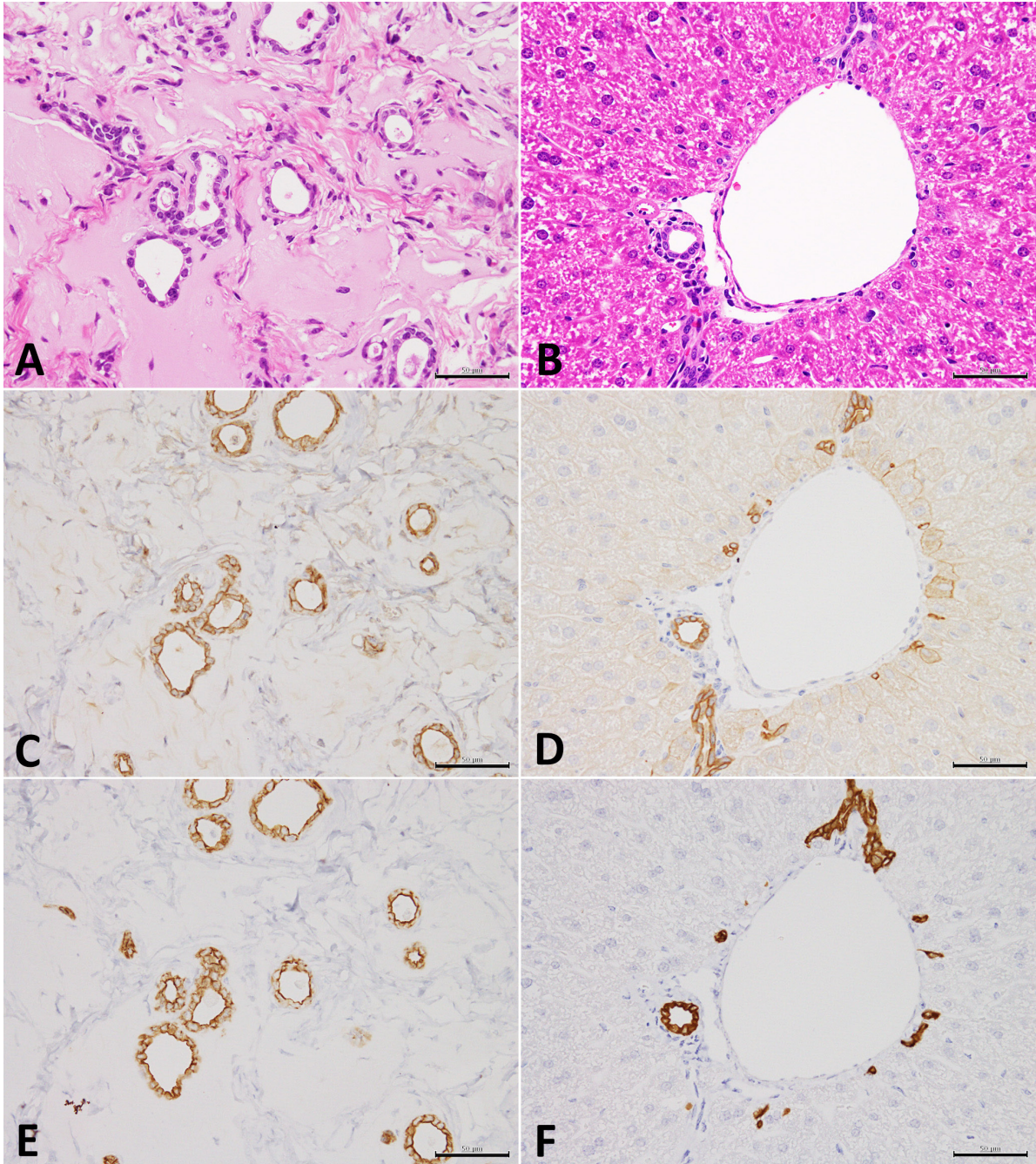


Fig. 6. (A) Microscopic appearance of Matrigel plugs in the nude mouse subcutis after injection of male B6J wild type mouse-derived normal liver (intrahepatic bile duct) organoids. Retained round glandular organoids are observed in interstitial tissue filled with retained Matrigel. H&E staining, bar=50 µm. (B) Normal hepatic cell cord and interlobular ductule/vessel appearance in a mouse strain identical to (A). H&E staining, bar=50 µm. (C) A serial section of (A) immunohistochemically stained for CK18. (D) A serial section of (B) immunohistochemically stained for CK18. (E) A serial section of (A) with immunohistochemically stained for CK19. Submembranous reactions for CK18/CK19 can be observed in organoid cells. (F) A serial section of (B) immunohistochemically stained for CK19. Cytoplasmic reactions in bile ducts and submembranous reactions in hepatocytes for CK18 can be observed. B6J: C57BL/6J; H&E: hematoxylin and eosin; CK: cytokeratin.

ment. Lesions with multilayered and/or invasive epithelial cells can be evaluated in hematoxylin and eosin-stained sections, but immunohistochemistry for CKs or oncogenic

kinases is more useful for accurate diagnosis and molecular evaluation.

CK Immunohistochemistry Assisted Evaluation of Multilayered Epithelia/Invasive Changes in Chemically Treated Organoids

CK composition varies depending on the epithelial cell type (simple vs. stratified), cellular growth state (normal vs. hyperproliferative), stage of development, differentiation program, and disease state²⁷. All human CKs can be divided into acidic (type I subfamily; CKs 9-20, partly react with the AE1 antibody) and basic (type II subfamily; CKs 1-8; react with the AE3 antibody) CKs, and they exist with specific pairing of type I and type II subfamilies into a heterotypic tetramer in almost all epithelial tissues^{27, 28}. The tissue-specific distribution of CKs in human tissues is highly similar to that in mouse tissues, with several exceptions²⁹.

Primary antibodies used for CK and α -smooth muscle actin (α SMA) immunohistochemistry, specimen pretreatment, and signal detection methods have been previously described²². To detect epithelial cell-derived changes in the Matrigel plugs and organoid-derived tissues, an anti-mouse CK19 rabbit monoclonal antibody (clone EPNCIR127B, Abcam, Cambridge, UK) was used after antigen retrieval in an autoclave in Tris-EDTA buffer (pH 9.0), which was suitable for minimizing background staining.

Both lung and liver organoids (intrahepatic bile duct) were CK19 positive. Therefore, in the evaluation of carcinogenicity of chemicals using the mouse normal tissue-derived organoid-based carcinogenesis model, multilayered and/or invasive epithelial cells were clearly visualized following immunohistochemical staining for CK19 (Figs. 3C and 5C). In contrast, monolayered epithelial cells clearly demarcated from the surrounding Matrigel/interstitium were observed in the untreated control groups (Figs. 4C and 6C). Accordingly, CK19 immunohistochemistry was useful for confirming the multilayered epithelia and distribution of extraductal invasive lesions for accurate diagnosis in the early stages of carcinogenesis. Immunohistochemistry for CKs other than CK19 was also performed in three organs/tissues. In this case, normal lung and liver tissues excised from male B6J mice and mammary tissue from female heterogeneous BALB/c-*Trp53* knockout or wild-type mice at 5 weeks of age (at which age organs/tissues for organoid culture were collected in our laboratory) were used. FFPE sections were prepared for comparative evaluation of organoids and normal organs/tissues.

Lung: Bronchiolar columnar cells and some cuboidal alveolar epithelial cells, which were presumed to be type 2 alveolar cells, were positive for CK19 and weakly positive for CK18 (Table 1, Fig. 4D–4F)³⁰. Both CKs exhibited typical submembranous and perinuclear localization. Pulmonary epithelial cells were negative for CK14. Immunohistochemistry for CKs in Matrigel plugs in nude mouse subcutis revealed positive reactions similar to normal lung tissues, that is, positive for CK19 and weakly positive for

Table 1. Immunohistochemical Localization of Epithelial Markers in Major Murine Organs/Tissues

Organ/Tissue	CK18	CK19	CK14	α SMA
Lung				
Bronchiolar epithelia	+	++	–	NT
Alveolar epithelia	+	++	–	NT
Liver				
Intrahepatic bile ducts	+	++	–	NT
Hepatocytes	+	–	–	NT
Mammary				
Ductal epithelia	++	++	–	–
Alveolar luminal cells	++	++	–	–
Myoepithelial cells	–	–	~++	+~++

–: negative; +: weakly positive; ++: positive; NT: not tested.

CK18, supporting their bronchiolar-alveolar cell origin²¹ (Fig. 4B, 4C). Normal lung tissue-derived organoids were characterized by scattered ciliated epithelia (Fig. 4A), further demonstrating their origin.

Liver: The intrahepatic bile ducts were positive for CK19 and weakly positive for CK18 (Table 1, Fig. 6D–6F). Weak immunoreactivity for CK18 was also observed in hepatocytes, as previously reported³¹. Liver-derived organoid cells, which were cultured in appropriately prepared media for differentiation into bile ducts²¹, were positive for CK19 and weakly positive for CK18 after their injection into nude mouse subcutis (Fig. 6B, 6C), supporting their intrahepatic bile duct epithelial cell origin. Bile ducts and hepatocytes were negative for CK14.

Mammary tissue: The mammary epithelium consists of subtypes of luminal (ductal and alveolar luminal cells) and myoepithelial cells³². In normal mammary tissues, the mammary ducts and glands are surrounded by adipose tissue (Fig. 7C). Immunohistochemistry revealed that the ductal/alveolar luminal cells were positive for CK18 and CK19 (Table 1, Fig. 7D), and the myoepithelial cells were positive for α SMA and CK14 (Fig. 7E and 7F). Mammary organoid cells in Matrigel plugs in nude mouse subcutis were positive for CK18 and CK19²². In contrast, the number of organoids containing α SMA- and/or CK14-positive cells was lower than that of the original mammary tissues (Fig. 7A and 7B), suggesting that ductal/alveolar luminal cells were predominantly cultured under previously reported culture conditions²¹. However, in the DMBA-induced adenocarcinoma developed after injection of BALB/c-heterozygous *Trp53* knockout mouse-derived mammary organoids into the nude mouse subcutis, not only CK19-positive carcinoma cells but also α SMA-positive cells were found surrounding the CK19-positive carcinoma cells (Fig. 2E and 2F). This suggested that both the CK19-positive luminal cells and the α SMA-positive myoepithelial cells were genetically altered by *in vitro* DMBA treatment, resulting in carcinoma formation comprising both types of carcinoma cells²².

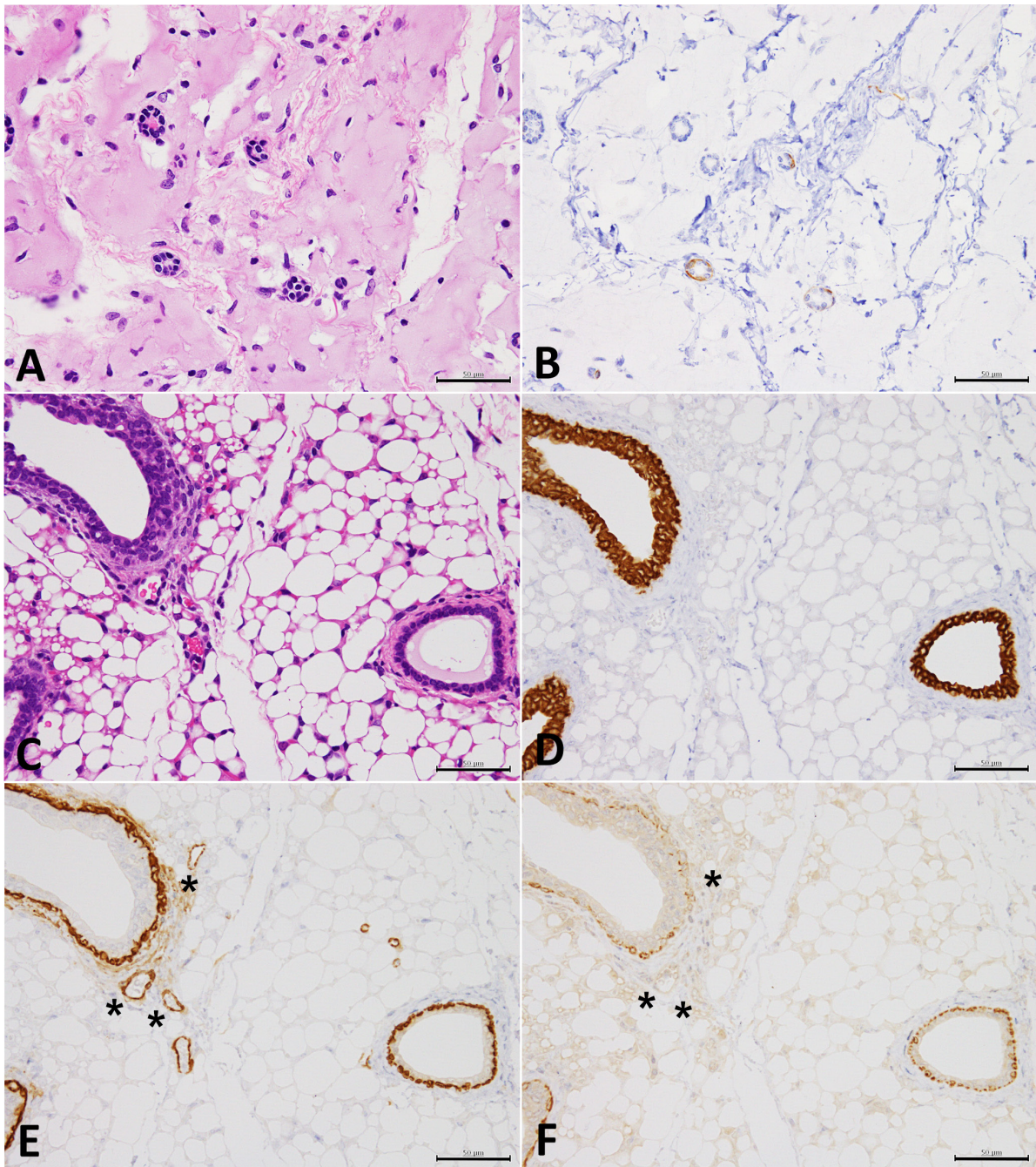


Fig. 7. (A) Matrigel plugs in the nude mouse subcutis after injection of female BALB/c wild type mouse-derived normal mammary organoids. H&E staining, bar=50 μm. (B) A serial section of (A) immunohistochemically stained for αSMA. (C) Normal immature mammary gland/duct surrounded by adipose tissue in a same mouse strain identical to (A). H&E staining, bar=50 μm. (D) A serial section of (C) immunohistochemically stained for CK19. Ductal and alveolar luminal cells showing strong cytoplasmic positivity can be observed. (E) A serial section of (C) immunohistochemically stained for αSMA. Positive myoepithelial cells surrounding ducts and glands can be observed. Note vascular walls are also positive for αSMA (asterisk). (F) A serial section of (C) immunohistochemically stained for CK14. Ductular myoepithelial cells are positive and glandular myoepithelial cells are partly positive for CK14. Note, vascular walls are CK14 negative (asterisk). H&E: hematoxylin and eosin; CK: cytokeratin; αSMA: α smooth muscle actin.

Expression of Oncogenic Kinases Indicated Molecular Activation of Epithelia in the Early Stages of Chemical Carcinogenesis

Protein kinases regulate key processes in cell activities such as cellular proliferation, survival, and migration. Therefore, it is well recognized that dysregulation of protein kinases due to genetic and epigenetic changes plays a role in many hallmarks of cancer³³. In the present review, two principal oncogenic kinases were selected as immunohistochemical markers, phospho-extracellular signal-regulated kinase (p-ERK) 1/2 and phospho-v-akt murine thymoma viral oncogene homolog (p-Akt), demonstrating that certain histopathological changes are associated with an early phase of carcinogenesis.

Extracellular signal-regulated kinase (ERK) is a member of the mammalian family of mitogen-activated protein kinases (MAPKs), and the ERK signaling pathway plays a key role in several steps of tumorigenesis, including cancer cell proliferation, migration, and invasion³⁴. This pathway is a convergent signaling node that receives input from numerous stimuli, including internal metabolic stress, DNA damage pathways, and altered protein concentrations, in addition to signals from external growth factors, cell-matrix interactions, and communication between cells³⁵. Furthermore, several mutations involving the MAPK/ERK pathway, such as those in the epithelial growth factor receptor gene (*EGFR*), *RAS*, and *BRAF*, have been identified as drivers of carcinogenesis³⁵. No mutations in genes encoding ERK kinases (*MAPK1* and *MAPK2*) have been reported as drivers of human cancers, but mutations in *RAS* and *RAF* oncogenes promote human cancers through phosphorylation of ERK kinases, which leads to their activation³⁶. The anti-phospho-ERK1 (T202/Y204) and ERK2 (T185/Y187) rabbit polyclonal antibodies from R&D Systems (AF1018; Minneapolis, MN, USA), and an avidin-biotin peroxidase method (Histofine, SAB-PO, Nichirei Biosciences, Tokyo, Japan) were used to assess the expression and localization of the antigens using immunohistochemistry. Antigen retrieval was conducted in an autoclave in citrate buffer (pH 6.0) prior to the immunoreactions. In EMS-induced adenocarcinoma developed due to injection of BALB/c-heterozygous *Trp53* knockout mouse-derived liver (intrahepatic bile duct) organoids, nuclear positivity for p-ERK1/2 was clearly observed (Fig. 2B), demonstrating that activation of the MAPK/ERK pathway is involved in carcinogenesis. In the case of EMS-treated lung organoids derived from the same mouse strain, focal nuclear positivity for p-ERK1/2 was observed in the multilayered epithelia (Fig. 3D) after the injection of this organoid into nude mouse subcutis, but the number of cells and areas with positive reaction were limited. The results suggested that EMS-induced early stage changes in carcinogenesis were observed after injection of the less sensitive lung organoids by p-ERK1/2-immunohistochemistry in contrast to the changes observed after injection of more sensitive liver (intrahepatic bile duct) organoids. No reactions were observed in the multilayered epithelia

from DEN-treated liver (intrahepatic bile duct) organoids of B6J-heterozygous *Trp53* knockout mice (Fig. 5D) after their injection, suggesting that DEN-induced carcinogenesis is associated with signaling pathways other than the MAPK/ERK pathway. No p-ERK1/2 positivity was observed in the untreated control group (data not shown).

AKT is a serine/threonine kinase and oncogenic protein that regulates cell survival, proliferation, growth, apoptosis, and glycogen metabolism³⁷. AKT is activated by phosphorylation at Thr308 or Ser473 and its induction interferes with normal regulatory mechanisms activating mTOR³⁷. An anti-phospho-Akt (Ser473) rabbit monoclonal antibody from Cell Signaling Technology (clone D9E, #4060; Danvers, MA, USA) and a one-step immunohistochemistry method (SignalStain Boost IHC Detection Reagent, Cell Signaling Technologies) were used to assess the expression and localization of the antigens. Antigen retrieval was conducted in an autoclave in citrate buffer (pH 6.0) prior to the immunoreactions. In EMS-induced adenocarcinoma from BALB/c-heterozygous *Trp53* knockout mouse-derived liver (intrahepatic bile duct) organoids, apical surface/cytoplasmic positivity for p-Akt was observed (Fig. 2C), demonstrating that activation of the Akt pathway was partially involved in carcinogenesis. Focal cytoplasmic positivity (Fig. 3E) and partial cytoplasmic positivity (Fig. 5E) were observed in the multilayered epithelia of EMS-treated lung organoids from BALB/c heterozygous *Trp53* knockout mice and DEN-treated liver (intrahepatic bile duct) organoids from B6J-heterozygous *Trp53* knockout mice. No p-Akt positivity was observed in the untreated control group (data not shown). Therefore, EMS- and DEN-induced carcinogenesis may be partly associated with Akt activation in an organoid-based carcinogenesis model.

Conclusion

In the present review, we discuss our current understanding of the histopathological and immunohistochemical characteristics of mouse normal tissue-derived organoids and tumors derived from these organoids after their *in vitro* treatment with genotoxic carcinogens and injection into nude mouse. In a recently reported organoid-based carcinogenesis model, normal lung/liver/mammary tissue-derived organoids from wild-type or heterogeneous BALB/c-*Trp53* knockout mice with B6J or BALB/c background were treated with several genotoxic carcinogens such as EMS and DEN. They exhibited macroscopic tumorigenicity as well as histopathological findings characteristic of the early stages of carcinogenesis, such as multilayered epithelia and/or invasive growth of epithelia. In contrast, simple glandular structures with monolayered epithelia were clearly demarcated from the surrounding Matrigel/interstitium in the untreated control groups. Clear immunohistochemical positivity for CK19 was observed in both lung bronchiolar-alveolar epithelial cells, intrahepatic bile ducts, and their organoid counterparts. Accordingly, CK19 immunohistochemistry was useful for confirming the multilayered epithelia and

distribution of extraductal invasive lesions for accurate diagnosis in the early stages of carcinogenesis. Immunohistochemistry for two principal oncogenic kinases, p-ERK 1/2 and p-Akt, suggested the molecular activation of epithelia in the early stages of chemical carcinogenesis depending on the carcinogen used. This review improves our biological understanding of organoid-based chemical carcinogenesis models. Further studies are required to identify other molecular markers indicating early stages in the organoid-based chemical carcinogenesis model to apply it to other organs/tissues and chemicals.

Disclosure of Potential Conflicts of Interest: The authors declare that there is no conflict of interest.

Acknowledgments: The authors would like to thank Ms. Ruri Nakanishi, and Ms. Yurika Shiotani (Central Animal Division National Cancer Center Research Institute, Tokyo, Japan) for their technical assistance. The authors would like to thank the Animal Core Facility of the National Cancer Center Research Institute for maintaining the mice, and for providing technical support with the histopathological evaluations. The Core Facility was supported by the National Cancer Center Research and Development Fund (2020J002). This study was supported a Health and Labor Sciences Research Grant from the Ministry of Health, Labour and Welfare of Japan (H30Food003).

References

- Huff J, and Haseman J. Long-term chemical carcinogenesis experiments for identifying potential human cancer hazards: collective database of the National Cancer Institute and National Toxicology Program (1976–1991). *Environ Health Perspect.* **96**: 23–31. 1991. [[Medline](#)] [[CrossRef](#)]
- Takaoka M, Sehata S, Maejima T, Imai T, Torii M, Satoh H, Toyosawa K, Tanakamaru ZY, Adachi T, Hisada S, Ueda M, Ogasawara H, Matsumoto M, Kobayashi K, Mutai M, and Usui T. Interlaboratory comparison of short-term carcinogenicity studies using CB6F1-rasH2 transgenic mice. *Toxicol Pathol.* **31**: 191–199. 2003. [[Medline](#)]
- Jacobson-Kram D. Cancer risk assessment approaches at the FDA/CDER: Is the era of the 2-year bioassay drawing to a close? *Toxicol Pathol.* **38**: 169–170. 2010. [[Medline](#)] [[CrossRef](#)]
- Tsutsumi H, Inoue R, Yasuda M, Takahashi R, Suzuki M, and Urano K. rasH2 mouse: reproducibility and stability of carcinogenicity due to a standardized production and monitoring system. *J Toxicol Pathol.* **35**: 19–24. 2022. [[Medline](#)] [[CrossRef](#)]
- Hisada S, Tsubota K, Inoue K, Yamada H, Ikeda T, and Sistare FD. Survey of tumorigenic sensitivity in 6-month rasH2-Tg mice studies compared with 2-year rodent assays. *J Toxicol Pathol.* **35**: 53–73. 2022. [[Medline](#)] [[CrossRef](#)]
- Ito N, Tamano S, and Shirai T. A medium-term rat liver bioassay for rapid in vivo detection of carcinogenic potential of chemicals. *Cancer Sci.* **94**: 3–8. 2003. [[Medline](#)] [[CrossRef](#)]
- Tanaka T, Kohno H, Suzuki R, Yamada Y, Sugie S, and Mori H. A novel inflammation-related mouse colon carcinogenesis model induced by azoxymethane and dextran sodium sulfate. *Cancer Sci.* **94**: 965–973. 2003. [[Medline](#)] [[CrossRef](#)]
- OECD/OCDE. Carcinogenicity studies. OECD guideline for the testing of chemicals. 451. 2018.
- Monro AM, and MacDonald JS. Evaluation of the carcinogenic potential of pharmaceuticals. Opportunities arising from the International Conference on Harmonisation. *Drug Saf.* **18**: 309–319. 1998. [[Medline](#)] [[CrossRef](#)]
- Sato T, Vries RG, Snippert HJ, van de Wetering M, Barker N, Stange DE, van Es JH, Abo A, Kujala P, Peters PJ, and Clevers H. Single Lgr5 stem cells build crypt-villus structures in vitro without a mesenchymal niche. *Nature.* **459**: 262–265. 2009. [[Medline](#)] [[CrossRef](#)]
- Sachs N, Papaspyropoulos A, Zomer-van Ommen DD, Heo I, Böttinger L, Klay D, Weeber F, Huelsz-Prince G, Iakobachvili N, Amatngalim GD, de Ligt J, van Hoeck A, Proost N, Viveen MC, Lyubimova A, Teeven L, Derakhshan S, Korving J, Begthel H, Dekkers JF, Kumawat K, Ramos E, van Oosterhout MF, Offerhaus GJ, Wiener DJ, Olimpio EP, Dijkstra KK, Smit EF, van der Linden M, Jaksani S, van de Ven M, Jonkers J, Rios AC, Voest EE, van Moorsel CH, van der Ent CK, Cuppen E, van Oudenaarden A, Coenjaerts FE, Meyaard L, Bont LJ, Peters PJ, Tans SJ, van Zon JS, Boj SF, Vries RG, Beekman JM, and Clevers H. Long-term expanding human airway organoids for disease modeling. *EMBO J.* **38**: 2019. [[Medline](#)] [[CrossRef](#)]
- Elbadawy M, Yamanaka M, Goto Y, Hayashi K, Tsunedomi R, Hazama S, Nagano H, Yoshida T, Shibutani M, Ichikawa R, Nakahara J, Omatsu T, Mizutani T, Katayama Y, Shinohara Y, Abugomaa A, Kaneda M, Yamawaki H, Usui T, and Sasaki K. Efficacy of primary liver organoid culture from different stages of non-alcoholic steatohepatitis (NASH) mouse model. *Biomaterials.* **237**: 119823. 2020. [[Medline](#)] [[CrossRef](#)]
- Little MH, and Combes AN. Kidney organoids: accurate models or fortunate accidents. *Genes Dev.* **33**: 1319–1345. 2019. [[Medline](#)] [[CrossRef](#)]
- Matsui T, and Shinozawa T. Human organoids for predictive toxicology research and drug development. *Front Genet.* **12**: 767621. 2021. [[Medline](#)] [[CrossRef](#)]
- Onuma K, Ochiai M, Orihashi K, Takahashi M, Imai T, Nakagama H, and Hippo Y. Genetic reconstitution of tumorigenesis in primary intestinal cells. *Proc Natl Acad Sci USA.* **110**: 11127–11132. 2013. [[Medline](#)] [[CrossRef](#)]
- Drost J, van Jaarsveld RH, Ponsioen B, Zimmerlin C, van Boxtel R, Buijs A, Sachs N, Overmeer RM, Offerhaus GJ, Begthel H, Korving J, van de Wetering M, Schwank G, Logtenberg M, Cuppen E, Snippert HJ, Medema JP, Kops GJ, and Clevers H. Sequential cancer mutations in cultured human intestinal stem cells. *Nature.* **521**: 43–47. 2015. [[Medline](#)] [[CrossRef](#)]
- Takeda H. A platform for validating colorectal cancer driver genes using mouse organoids. *Front Genet.* **12**: 698771. 2021. [[Medline](#)] [[CrossRef](#)]
- Matsuura T, Maru Y, Izumiya M, Hoshi D, Kato S, Ochiai M, Hori M, Yamamoto S, Tatsuno K, Imai T, Aburatani H, Nakajima A, and Hippo Y. Organoid-based ex vivo reconstitution of Kras-driven pancreatic ductal carcinogenesis. *Carcinogenesis.* **41**: 490–501. 2020. [[Medline](#)] [[CrossRef](#)]
- Murakami K, Terakado Y, Saito K, Jomen Y, Takeda H,

- Oshima M, and Barker N. A genome-scale CRISPR screen reveals factors regulating Wnt-dependent renewal of mouse gastric epithelial cells. *Proc Natl Acad Sci USA*. **118**: 2021. [[Medline](#)] [[CrossRef](#)]
20. Kasuga A, Semba T, Sato R, Nobusue H, Sugihara E, Takaiishi H, Kanai T, Saya H, and Arima Y. Oncogenic KRAS-expressing organoids with biliary epithelial stem cell properties give rise to biliary tract cancer in mice. *Cancer Sci*. **112**: 1822–1838. 2021. [[Medline](#)] [[CrossRef](#)]
 21. Naruse M, Masui R, Ochiai M, Maru Y, Hippo Y, and Imai T. An organoid-based carcinogenesis model induced by in vitro chemical treatment. *Carcinogenesis*. **41**: 1444–1453. 2020. [[Medline](#)] [[CrossRef](#)]
 22. Naruse M, Ishigamori R, and Imai T. The unique genetic and histological characteristics of DMBA-induced mammary tumors in an organoid-based carcinogenesis model. *Front Genet*. **12**: 765131. 2021. [[Medline](#)] [[CrossRef](#)]
 23. Rabata A, Fedr R, Soucek K, Hampl A, and Koledova Z. 3D cell culture models demonstrate a role for FGF and WNT signaling in regulation of lung epithelial cell fate and morphogenesis. *Front Cell Dev Biol*. **8**: 574. 2020. [[Medline](#)] [[CrossRef](#)]
 24. Maru Y, Onuma K, Ochiai M, Imai T, and Hippo Y. Shortcuts to intestinal carcinogenesis by genetic engineering in organoids. *Cancer Sci*. **110**: 858–866. 2019. [[Medline](#)] [[CrossRef](#)]
 25. Sato T, Morita M, Tanaka R, Inoue Y, Nomura M, Sakamoto Y, Miura K, Ito S, Sato I, Tanaka N, Abe J, Takahashi S, Kawai M, Sato M, Hippo Y, Shima H, Okada Y, and Tanuma N. *Ex vivo* model of non-small cell lung cancer using mouse lung epithelial cells. *Oncol Lett*. **14**: 6863–6868. 2017. [[Medline](#)]
 26. Ochiai M, Yoshihara Y, Maru Y, Tetsuya M, Izumiya M, Imai T, and Hippo Y. Kras-driven heterotopic tumor development from hepatobiliary organoids. *Carcinogenesis*. 2019. [[Medline](#)] [[CrossRef](#)]
 27. Cooper D, Schermer A, and Sun TT. Classification of human epithelia and their neoplasms using monoclonal antibodies to keratins: strategies, applications, and limitations. *Lab Invest*. **52**: 243–256. 1985. [[Medline](#)]
 28. Hatzfeld M, and Franke WW. Pair formation and promiscuity of cytokeratins: formation in vitro of heterotypic complexes and intermediate-sized filaments by homologous and heterologous recombinations of purified polypeptides. *J Cell Biol*. **101**: 1826–1841. 1985. [[Medline](#)] [[CrossRef](#)]
 29. Martín CA, Salomoni PD, and Badrán AF. Cytokeratin immunoreactivity in mouse tissues: study of different antibodies with a new detection system. *Appl Immunohistochem Mol Morphol*. **9**: 70–73. 2001. [[Medline](#)]
 30. Yi H, and Ku NO. Intermediate filaments of the lung. *Histochem Cell Biol*. **140**: 65–69. 2013. [[Medline](#)] [[CrossRef](#)]
 31. Park JE, Kim HT, Lee S, Lee YS, Choi UK, Kang JH, Choi SY, Kang TC, Choi MS, and Kwon OS. Differential expression of intermediate filaments in the process of developing hepatic steatosis. *Proteomics*. **11**: 2777–2789. 2011. [[Medline](#)] [[CrossRef](#)]
 32. Visvader JE. Keeping abreast of the mammary epithelial hierarchy and breast tumorigenesis. *Genes Dev*. **23**: 2563–2577. 2009. [[Medline](#)] [[CrossRef](#)]
 33. Fleuren ED, Zhang L, Wu J, and Daly RJ. The kinome ‘at large’ in cancer. *Nat Rev Cancer*. **16**: 83–98. 2016. [[Medline](#)] [[CrossRef](#)]
 34. Kim EK, and Choi EJ. Pathological roles of MAPK signaling pathways in human diseases. *Biochim Biophys Acta*. **1802**: 396–405. 2010. [[Medline](#)] [[CrossRef](#)]
 35. Burotto M, Chiou VL, Lee JM, and Kohn EC. The MAPK pathway across different malignancies: a new perspective. *Cancer*. **120**: 3446–3456. 2014. [[Medline](#)] [[CrossRef](#)]
 36. Deschênes-Simard X, Kottakis F, Meloche S, and Ferbeyre G. ERKs in cancer: friends or foes? *Cancer Res*. **74**: 412–419. 2014. [[Medline](#)] [[CrossRef](#)]
 37. Song M, Bode AM, Dong Z, and Lee MH. AKT as a therapeutic target for cancer. *Cancer Res*. **79**: 1019–1031. 2019. [[Medline](#)] [[CrossRef](#)]